

1           **Early detection of SARS-CoV-2 in circulating immune cells in a mouse model**

2           Tingting Geng<sup>1\*</sup>, Spencer Keilich<sup>2\*</sup>, Triantafyllos Tafas<sup>2</sup>, Penghua Wang<sup>1</sup>

3  
4   <sup>1</sup> Department of Immunology, School of Medicine, University of Connecticut Health Center,  
5 Farmington, CT 06030, USA

6   <sup>2</sup> QCDx LLC, 400 Farmington Ave, Farmington, CT 06032, USA.

7  
8   \* T.G. and S.K. contributed equally

9  
10 Address correspondence to:

11 Penghua Wang, Ph.D., Department of Immunology, School of Medicine, University of  
12 Connecticut Health Center, Farmington, CT 06030, USA. Email: [pewang@uchc.edu](mailto:pewang@uchc.edu), Tel: 860-  
13 679-6393.

14 Triantafyllos Tafas Ph.D., QCDx LLC, 400 Farmington Ave, Farmington, CT 06032. Email:  
15 [fyl.tafas@qcd-x.com](mailto:fyl.tafas@qcd-x.com), Tel: 860-679-4673.

16  
17 Word count for the abstract: 98

18 Word count for the main text: 1992

19

20 **Footnote**

21

22 **Conflict of Interest:** T.G. and P.W. declare no competing financial interest. S.K. and T.T. are  
23 employed by QCDx LLC.

24

25 **Funding Source:** National Institutes of Health grant R01AI132526 to P.W.

26 University of Connecticut Health Center grant G401894 to P.W.

27

28 **Previous presentation:** None

29

30 **Corresponding Author Contact Information:** Penghua Wang, Ph.D., 263 Farmington Avenue,  
31 Farmington, CT 06030; Tel: 860-679-6393; Email: [pewang@uchc.edu](mailto:pewang@uchc.edu)

32 **ABSTRACT**

33 SARS-CoV-2 infects the respiratory tract, lung and then other organs. However, its  
34 pathogenesis remains largely unknown. We used RareScope™ Fluorescence Light Sheet  
35 Microscopy (FLSM) and fluorescent in situ hybridization of RNA (RNA-FISH) to detect SARS-  
36 CoV-2 RNA and dissemination kinetics in mouse blood circulation. By RNA-FISH, we found  
37 that SARS-CoV-2 RNA-positive leukocytes, including CD11c cells, appeared as early as one  
38 day after infection and continued through day 10 post infection. Our data suggest that SARS-  
39 CoV-2-permissive leukocytes contribute to systemic viral dissemination, and RNA-FISH  
40 combined with FLSM can be utilized as a sensitive tool for SARS-CoV-2 detection in blood  
41 specimens.

42

43 **Key words:** SARS-CoV-2, viral, pathogenesis, RNA-FISH, FLSM, detection

## 44 **Background**

45 The (+) single-stranded (ss) RNA coronaviruses (CoV) are major cause of fatal human  
46 respiratory diseases, such as Severe Acute Respiratory Syndrome (SARS)-causing CoV and  
47 Middle East Respiratory Syndrome (MERS)-CoV. SARS started in November 2002 in Southern  
48 China, spread to 26 countries, and resulted in 8439 cases and 821 deaths[1]. Between its  
49 discovery in 2012 and January 2020, MERS-CoV caused 2519 cases and 866 deaths[2]. At the  
50 end of 2019, a new SARS strain, SARS-CoV-2, which is 86% identical to SARS-CoV-1 at the  
51 amino residue level, emerged in humans in Central China and now has spread worldwide. As of  
52 today, there are >34 million confirmed SARS-CoV-2 cases and >1 million deaths from ~250  
53 countries[3], constituting the greatest global public health crisis in the 21<sup>st</sup> century.

54         Once a human SARS-CoV gains entry through the respiratory tract, airway epithelial  
55 cells, alveolar epithelial cells, vascular endothelial cells and alveolar macrophages are among  
56 the first target [4, 5]. These cell types are suspected to be 'ground-zero' for early infection and  
57 subsequent replication [6, 7]. In particular, proinflammatory monocyte-derived macrophages  
58 were dominant in the bronchoalveolar lavage fluid from patients with severe COVID-19 [8].  
59 These SARS-CoV-2 permissive cells could contribute to lung inflammation and viral  
60 dissemination to other organs.

61 We here employed a mouse model and RareScope™ Fluorescence Light Sheet Microscopy  
62 (FLSM) to examine early dissemination of SARS-CoV-2 through the blood circulation. We report  
63 that SARS-CoV-2 positive leukocytes appear early after infection, which could help this virus  
64 spread systemically.

## 65 **Methods**

### 66 *Cell and virus culture*

67 Vero cells (monkey kidney epithelial cells, Cat. # CCL-81) were purchased from ATCC  
68 (Manassas, VA, USA). The cells were grown at 37°C and 5% CO<sub>2</sub> in complete DMEM medium:  
69 Dulbecco's modified Eagle medium (DMEM) (Corning) supplemented with 10% fetal bovine  
70 serum (FBS) (Gibco) and 1% penicillin-streptomycin (P/S; Corning). These cell lines are not  
71 listed in the database of commonly misidentified cell lines maintained by ICLAC, and in our  
72 hands tested negative for mycoplasma contamination. In order to ensure cell cultures are  
73 mycoplasma free, we regularly treated cells with MycoZap (Lonza). SARS-CoV-2 (NR-52281  
74 SARS-related coronavirus 2, isolate USA-WA1/2020) was propagated in Vero cells and  
75 concentrated with a polyethylene glycol (PEG) (Cat# LV-810A, System Biosciences, Palo Alto,  
76 CA 94303, USA) to a titer of  $\sim 1 \times 10^7$  plaque forming units (PFU)/ml. Adeno 5 virus expressing  
77 the receptor for SARS-CoV-2, human Angiotensin Converting Enzyme 2 (hACE2) was custom-  
78 made by VectorBuilder Inc. (Chicago, IL 60609, USA).

79

### 80 *Mouse infection and sample collection*

81 Mouse experiments were approved and performed according to the guidelines of  
82 the Institutional Animal Care and Use Committee at Yale University. 8-10 weeks-old female  
83 C57BL/6J mice (JAX Stock #: 000664) were inoculated with  $2 \times 10^8$  PFU of Ad5-hACE2 by  
84 intranasal instillation. Five days after Ad5 transduction, three mice were subsequently infected  
85 with  $2 \times 10^5$  PFU of SARS-CoV-2 through the intranasal route in the BSL-3 facility at Yale  
86 University, New Haven, CT. Whole blood was collected retro-orbitally at different time point after  
87 anesthesia using 30%v/v isoflurane diluted in propylene glycol. Approximately 100  $\mu$ l whole  
88 blood were collected for RNA-FISH and 50  $\mu$ l for RNA isolation and Quantitative PCR (qPCR).  
89 For tissue collection, mice were euthanized in 100% Isoflurane. About 20mg of left lung tissue  
90 was harvested at the indicated time point for western, and 20 mg of left lung tissue for RNA

91 isolation and qPCR. Day 0 mouse samples were taken from uninfected animals collected and  
92 isolated in the same manner with Ad5 transduction.

93

#### 94 *RNA-FISH and RareScope™ Fluorescence Light Sheet Microscopy*

95 An RNA FISH probe was developed against the SARS-CoV-2 Spike gene. The probe  
96 was designed based on the published SARS-CoV-2 genome  
97 (<https://www.ncbi.nlm.nih.gov/nucore/MN985325>) and consists of 48 individual oligomer-  
98 primers, custom-built by Cambridge Bioscience (Cambridge, CB23 8SQ, United Kingdom)  
99 (**Supplementary Table 1**). The full Spike RNA target sequence is 1,673nt in length and the  
100 chosen oligomers cover independent 20nt sequences. The 48 oligomers underwent basic local  
101 alignment search tool (BLAST) analysis to eliminate off-target hybridization. Each oligomer has  
102 a fluorescent tail of Quasar 670 (LGC Biosearch Technologies, Middlesex, UK). All white blood  
103 cells (WBCs) from each mouse and each time-point blood samples were fluorescently  
104 immunostained in solution. Signals for 5 fluorescent markers were created by staining with  
105 antibodies against the common leukocyte antigen (Rat-anti-mouse CD45, Cat# 550539, clone:  
106 30-F11, BD Pharmingen, San Jose, CA 95131, USA) indirectly labeled with a goat-anti-rat  
107 secondary antibody labeled with Alexa Fluor 488, a dendritic cell anti-CD11c marker (Hamster-  
108 anti-Mouse CD11c, Cat# 553799, clone HL3, BD Pharmingen) indirectly labeled with goat-anti-  
109 Hamster Alexa Fluor 594, hACE2 (Mouse-anti-Human ACE-2, Cat# sc-390851, clone E-11,  
110 Santa Cruz Biotechnology) indirectly labeled with goat-anti-mouse Alexa Fluor 594, and the  
111 RNA-FISH Spike Probe fluorescently labeled with Quasar 670. Nuclei were counterstained by  
112 Hoechst 33342.

113 After staining, the morphologically intact cells were immobilized in hydrogel into  
114 RarePrep™ specimen fixtures that were loaded in the RareScope 4D (X, Y, Z and rotational)  
115 microscope stage for 3-dimensional (3-D) imaging. The RarePrep fixture presents the cylindrical,  
116 transparent suspension of immobilized cells to the RareScope FLSM optical path where it is

117 scanned in an automated fashion. Utilizing proprietary script programs created on the  
118 Fiji/ImageJ software platform, 3-D image stacks of the immobilized cells are acquired,  
119 individually for each of the 5 fluorescent markers. The 3-D image stacks from each blood  
120 sample were analyzed by expert reviewers and more than five hundred WBCs counted to verify  
121 presence of SARS-CoV-2 signals, totaling 1500-2000 cells from each mouse and each time-  
122 points.

123

#### 124 *RNA extraction and Quantitative reverse-transcription PCR*

125 Total RNA was isolated from whole blood and lung tissue using a PureLink RNA Mini kit  
126 (Invitrogen, Germantown, MD 20874, USA). All the blood and tissue samples were kept in RNA  
127 Lysis Buffer in -80% before RNA purification. Reverse transcription was performed using a  
128 PrimeScript™ RT Reagent Kit (Takara Bio, Mountain View, CA 94043 USA). qPCR was  
129 performed with gene specific primers and SYBR Green (iTaQ Universal SYBR Green Supermix,  
130 Bio-Rad, Hercules, CA 94547, USA). The primers for SARS-CoV-2 were published by the  
131 Centers for Disease Control and Prevention of United States of America: forward primer (5'-  
132 GAC CCC AAA ATC AGC GAA AT -3') and reverse primer (5'- TCT GGT TAC TGC CAG TTG  
133 AAT CTG -3'). The primers for hACE2 were forward primer (5'-  
134 ATCTGAGGTCGGCAAGCAGC-3') and reverse primer (5'-CAATAATCCCCATAGTCCTC-3').  
135 The primers for the housekeeping gene control mouse beta actin, Actb, where: forward primer  
136 (5'- AGAGGGAAATCGTGCGTGAC -3') and reverse primer (5'-  
137 CAATAGTGATGATGACCTGGCCGT-3'). The following PCR cycling program was used: 10 min  
138 at 95°, and 40 cycles of 15 sec at 95° and 1 min at 60°C.

139

140

## 141 RESULTS

142 SARS-CoV-2 is transmitted primarily through respiratory droplets, infects the respiratory  
143 tract, lung and then disseminates to other organs likely through the blood circulation. However,  
144 its dissemination kinetics are unknown. To this end, we tested if SARS-CoV-2 positive white  
145 blood cells could be detected using a mouse model. Generally speaking, human SARS-CoV-2  
146 does not infect efficiently or cause overt disease in mice [9]. However, human ACE2 (hACE2, a  
147 major cellular entry receptor for SARS-CoV-2)-transgenic [9] or transiently transduced mice are  
148 susceptible to SARS-CoV-2 infection and develop lung pathology [10]. Thus, we transiently  
149 expressed human ACE2 in mice using a non-replicating adenovirus 5 vector and then infected  
150 them with SARS-CoV-2. hACE2 expression and SARS-CoV-2 are largely restricted to mouse  
151 lungs [10]. In our Ad5-hACE2 mouse model, hACE2 was successfully expressed in lung tissue  
152 (**Fig. 1A**), and SARS-CoV-2 was positive in lung after 4 days of infection (**Fig. 1B**). As a control,  
153 we first validated the SARS-CoV-2-RNA probe in heavily infected Vero cells (**Fig.1C**). Then, we  
154 included a human blood sample (without SARS-CoV-2 infection) as control in which hACE2 was  
155 expressed at a high level. SARS-CoV-2 + / CD45+ cells were detected in mice two days post  
156 infection (**Fig.1D**).

157 After validation of the mouse model and RNA-FISH probe, a cohort of 3 mice were  
158 tested longitudinally over a period of 8 days. Blood sample of 100  $\mu$ l each mouse was collected  
159 retro-orbitally before SARS-CoV-2 infection (0 DPI) and none of the three blood samples had  
160 SARS-CoV-2<sup>+</sup> Spike mRNA signatures in WBC (**Fig. 2A, 2B**). The same three mice were  
161 infected with SARS-CoV-2, and blood was collected on 1, 3, and 8 DPI. On the first day post  
162 infection (1 DPI), we observed that leukocytes were positive for SARS-CoV-2 Spike mRNA  
163 (1.08%), and SARS-CoV-2<sup>+</sup> cells increased slightly in frequency to a peak of about 1.27% on 3  
164 DPI and then declined to about 0.28% on 8 DPI (**Fig. 2A, 2B**). There was a statistically  
165 significant difference between groups, based on Single Factor ANOVA ( $F(4,12) = 17.39$ ,  
166  $p = .0007$ ) comparing the change in mean frequency of spike positive cells overtime. The Spike



167 mRNA signal was robust with diverse morphology ranging from well-defined FISH dots to  
168 disperse clouds of SARS-CoV-2 signal positivity in CD45 and CD11c positive cells (**Fig. 2C**).  
169 Another 50µl of whole blood was collected at the same time in the same cohort for RNA  
170 extraction and quantitative RT-PCR (qPCR) detection of SARS-CoV-2 RNA. No blood  
171 specimens tested positive for SARS-CoV-2 by qPCR with a cut off threshold cycle (Ct) set at 40  
172 (**Supplementary Table 2**).

173

## 174 **DISCUSSION**

175         Once the virus gains entry through the respiratory tract, the first cells to be infected are  
176 airway epithelial cells, alveolar epithelial cells, vascular endothelial cells and alveolar  
177 macrophages [4, 5]. SARS-CoV-2 may also infect immature and mature human monocyte-  
178 derived DCs [11]. Subsequently, viruses disseminate through the blood circulation to other  
179 permissive organs. We here demonstrated the presence of SARS-CoV-2 Spike mRNA-positive  
180 WBCs by RNA-FISH rapidly, at day 1 post infection (**Fig.2C**). Interestingly, a large portion of the  
181 SARS-CoV-2-carrying WBCs were innate CD11c-positive cells on 1 DPI. CD11c is most  
182 prominently expressed by dendritic cells, but also by monocytes, macrophages, neutrophils, and  
183 some B cells. Since in our mouse model SARS-CoV-2 infection is limited to the lung [10], these  
184 circulating SARS-CoV-2-positive immune cells are likely to have originated from immune  
185 infiltrates and/or resident immune cells in the lung. These cells could have been rapidly  
186 activated to produce innate antiviral immune responses, and to activate adaptive immunity,  
187 including dendritic cell trafficking to lymph nodes early in infection. Indeed, viral infection triggers  
188 rapid differentiation of human blood monocytes into dendritic cells (DCs) with enhanced  
189 capacity to activate T cells [12]. However, circulating SARS-CoV-2-positive DCs could help virus  
190 spread to other tissues. This has been observed in dengue virus infection, which depends on  
191 CD11b<sup>+</sup>, CD11c<sup>+</sup>, and CD45<sup>+</sup> cells for systemic dissemination [13]. Future work is needed to  
192 include more immunocyte markers to identify the different categories of WBC which contribute

193 to SARS-CoV-2 dissemination. We recognize that expression of hACE2 by an adenovirus  
194 vector may potentially alter the cell tropism of SARS-CoV-2 because of a broad cell tropism of  
195 adenoviruses. Nonetheless, our results still provide insight into early responsive immune cells  
196 and viral dissemination.

197 Another intriguing finding of this study is sensitive detection of SARS-CoV-2 by RNA-  
198 FISH coupled with RareScope microscopy. In our experimental conditions, SARS-CoV-2 RNA  
199 was undetectable in the blood throughout all time points. RNA-FISH coupled with RareScope  
200 microscopy method seems more sensitive for detection of SARS-CoV-2 in blood than RT-PCR.

201 The enhanced sensitivity of RNA-FISH-based detection is likely because, with  
202 RareScope-based detection, the cell morphology and viral RNA integrity are preserved in the  
203 cell suspension immobilized in a hydrogel. Furthermore, cumulative signals from 48 individual  
204 20 nt-oligomers in the SARS-CoV-2 probe targeting the viral Spike gene may increase  
205 sensitivity. A potential concern about RNA-FISH could be future mismatch between probes and  
206 the SARS-CoV-2 genome due to rapid mutation [14], which could be also a problem to qPCR  
207 with two primers. However, this problem can be overcome by timely sequencing of new clinical  
208 SARS-CoV-2 isolates. By far, the Spike gene is very well conserved among the clinical isolates  
209 worldwide [15]. Of note, even with a 48-oligomer probe, the RNA-FISH method demonstrated  
210 high specificity as all uninfected blood samples were negative for SARS-CoV-2 RNA. Therefore,  
211 our RNA-FISH method is likely a more robust diagnostic with blood specimens than qPCR.  
212 Future work is to test our method with clinical blood specimens of COVID-19 patients.

213

214 **Author contributions**

215 T.G. performed the animal and qPCR work; S.K. performed the RNA-FISH and microscopy. T.T.

216 and P.W. conceived and supervised the study. T.G., S.K., T.T. and P.W. wrote the manuscript.

217 All the authors reviewed and/or modified the manuscript.

218 We are thankful to Anthony T. Vella, Ph.D. for helping with textual editing.

219 **REFERENCES**

- 220 1. WHO. Cumulative Number of Reported Probable Cases of SARS.  
221 [https://www.who.int/csr/sars/country/2003\\_07\\_04/en/](https://www.who.int/csr/sars/country/2003_07_04/en/) **2003**.
- 222 2. WHO. Middle East respiratory syndrome coronavirus (MERS-CoV).  
223 <https://www.who.int/emergencies/mers-cov/en/> **2020**.
- 224 3. WHO. Coronavirus disease (COVID-2019) situation reports.  
225 <https://www.who.int/emergencies/diseases/novel-coronavirus-2019/situation-reports/> **2020**.
- 226 4. Jia HP, Look DC, Shi L, et al. ACE2 Receptor Expression and Severe Acute Respiratory  
227 Syndrome Coronavirus Infection Depend on Differentiation of Human Airway Epithelia. *Journal*  
228 *of Virology* **2005**; 79:14614–21.
- 229 5. Hamming I, Timens W, Bulthuis M, Lely A, Navis G, Goor Hv. Tissue distribution of ACE2  
230 protein, the functional receptor for SARS coronavirus. A first step in understanding SARS  
231 pathogenesis. *The Journal of Pathology* **2004**; 203:631–7.
- 232 6. Ziegler CGK, Allon SJ, Nyquist SK, et al. SARS-CoV-2 receptor ACE2 is an interferon-  
233 stimulated gene in human airway epithelial cells and is detected in specific cell subsets across  
234 tissues. *Cell* **2020**.
- 235 7. Li MY, Li L, Zhang Y, Wang XS. Expression of the SARS-CoV-2 cell receptor gene ACE2 in  
236 a wide variety of human tissues. *Infectious Diseases of Poverty* **2020**; 9.
- 237 8. Liao M, Liu Y, Yuan J, et al. Single-cell landscape of bronchoalveolar immune cells in  
238 patients with COVID-19. *Nature Medicine* **2020**.
- 239 9. Bao L, Deng W, Huang B, et al. The Pathogenicity of SARS-CoV-2 in hACE2 Transgenic  
240 Mice. *bioRxiv* **2020**:2020.02.07.939389.
- 241 10. Sun J, Zhuang Z, Zheng J, et al. Generation of a Broadly Useful Model for COVID-19  
242 Pathogenesis, Vaccination, and Treatment. *Cell* **2020**; 182:734-43 e5.

- 243 11. Yilla M, Harcourt BH, Hickman CJ, et al. SARS-coronavirus replication in human peripheral  
244 monocytes/macrophages. *Virus Res* **2005**; 107:93-101.
- 245 12. Hou W, Gibbs JS, Lu X, et al. Viral infection triggers rapid differentiation of human blood  
246 monocytes into dendritic cells. *Blood* **2012**; 119:3128-31.
- 247 13. Pham AM, Langlois RA, TenOever BR. Replication in cells of hematopoietic origin is  
248 necessary for Dengue virus dissemination. *PLoS Pathog* **2012**; 8:e1002465.
- 249 14. Shen Z, Xiao Y, Kang L, et al. Genomic Diversity of Severe Acute Respiratory Syndrome-  
250 Coronavirus 2 in Patients With Coronavirus Disease 2019. *Clin Infect Dis* **2020**; 71:713-20.
- 251 15. Pachetti M, Marini B, Benedetti F, et al. Emerging SARS-CoV-2 mutation hot spots include  
252 a novel RNA-dependent-RNA polymerase variant. *J Transl Med* **2020**; 18:179.
- 253

254 **FIGURE LEGENDS**

255 **Figure 1 Validation of the Ad5-hACE2 mouse model and RNA-FISH probe.**

256 **A)** Western blots of lung tissue from Ad5-hACE2 mouse and Ad5-Vec control mouse. **B)** qPCR  
257 quantification of SARS-CoV2 virus loads in lung tissue of Ad5-hACE2 mouse before and 4 days  
258 after SARS-CoV2 infection. **C)** Images of Vero cells as positive and negative experimental  
259 controls. Mock and infected Vero cells were stained with SARS-CoV2 RNA FISH and an  
260 epithelial immunofluorescent (IF) marker [pan-Cytokeratin (Pan-CK) specific for 18 different  
261 clones of Cytokeratin]. Vero composite images use blue for nucleus, green for pan-CK, and red  
262 for CoV-2 Spike RNA. **D)** Immunofluorescent images of white blood cells (WBC) from human  
263 and mouse. WBCs were fixed and stained for CD45 indirectly labeled with Alexa Fluor 488,  
264 human ACE2 indirectly labeled with Alexa Fluor 594 and the RNA-FISH Spike probe directly  
265 conjugated with Quasar 670. Nuclear DNA was counterstained by Hoechst 33342. The  
266 composite images are the combination of nuclear DNA (blue), CD45 (green), hACE2(yellow)  
267 and SAR-CoV-2 Spike RNA (Red). The images were acquired with a RareScope FLSM  
268 microscope with a water immersion 20X, NA 0.5 objective lens.

269

270 **Figure 2 Detection of SARS-CoV2 RNA in white blood cells by RNA-FISH.**

271 **A)** The percentage of SARS-CoV2-positive WBC. Bars: mean  $\pm$  s.e.m. Each (•) symbol = one  
272 animal. **B)** A summary of threshold cycle (Ct) of qPCR of SARS-CoV-2 RNA at different days  
273 post infection (DPI). Each row indicates one mouse blood sample with technical triplicate. Actb  
274 is a mouse house-keeping gene. N.A (not applicable): Ct greater than 40. **C)**  
275 Immunofluorescent images of white blood cells (WBC) from different days post infection (DPI).  
276 WBCs were fixed and stained for CD45 indirectly labeled with Alexa Fluor 488, goat-anti-  
277 hamster CD11c indirectly labeled with Alexa Fluor 594 and the RNA-FISH Spike probe directly  
278 conjugated with Quasar 670. Nuclear DNA was counterstained by Hoechst 33342. The  
279 composite images are the combination of nuclear DNA (blue), CD45 (green), CD11c(yellow)

280 and SAR-CoV-2 Spike RNA (Red). The images were acquired with a RareScope FLSM  
281 microscope with a water immersion 20X, NA 0.5 objective lens.

282 **Supplementary data**

283

284 **Table 1** The list of Quasar 670 Fluorescently labelled primers included in the RNA-FISH probe  
285 for the SARS-CoV2 Spike gene.

286

287 **Table 2** The total counts of SARS-CoV-2 Spike RNA positive cell in WBCs with the percent of  
288 Spike RNA positive cells out of total nuclei.



Fig.1

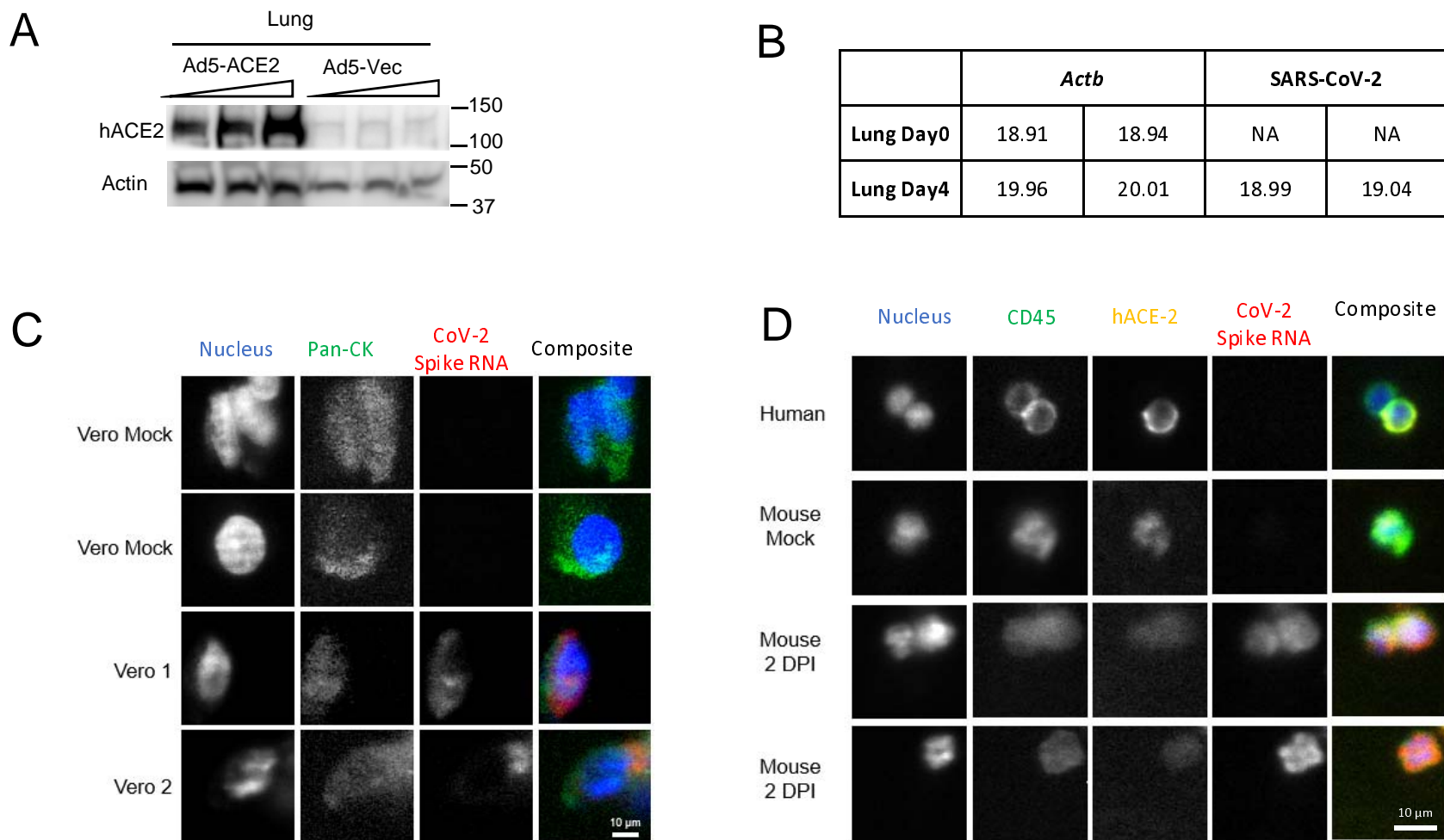
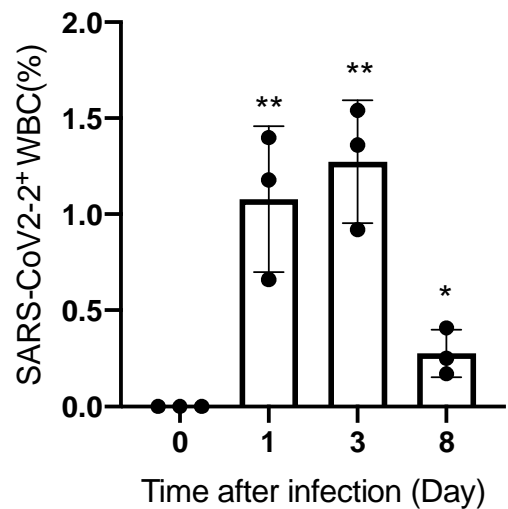
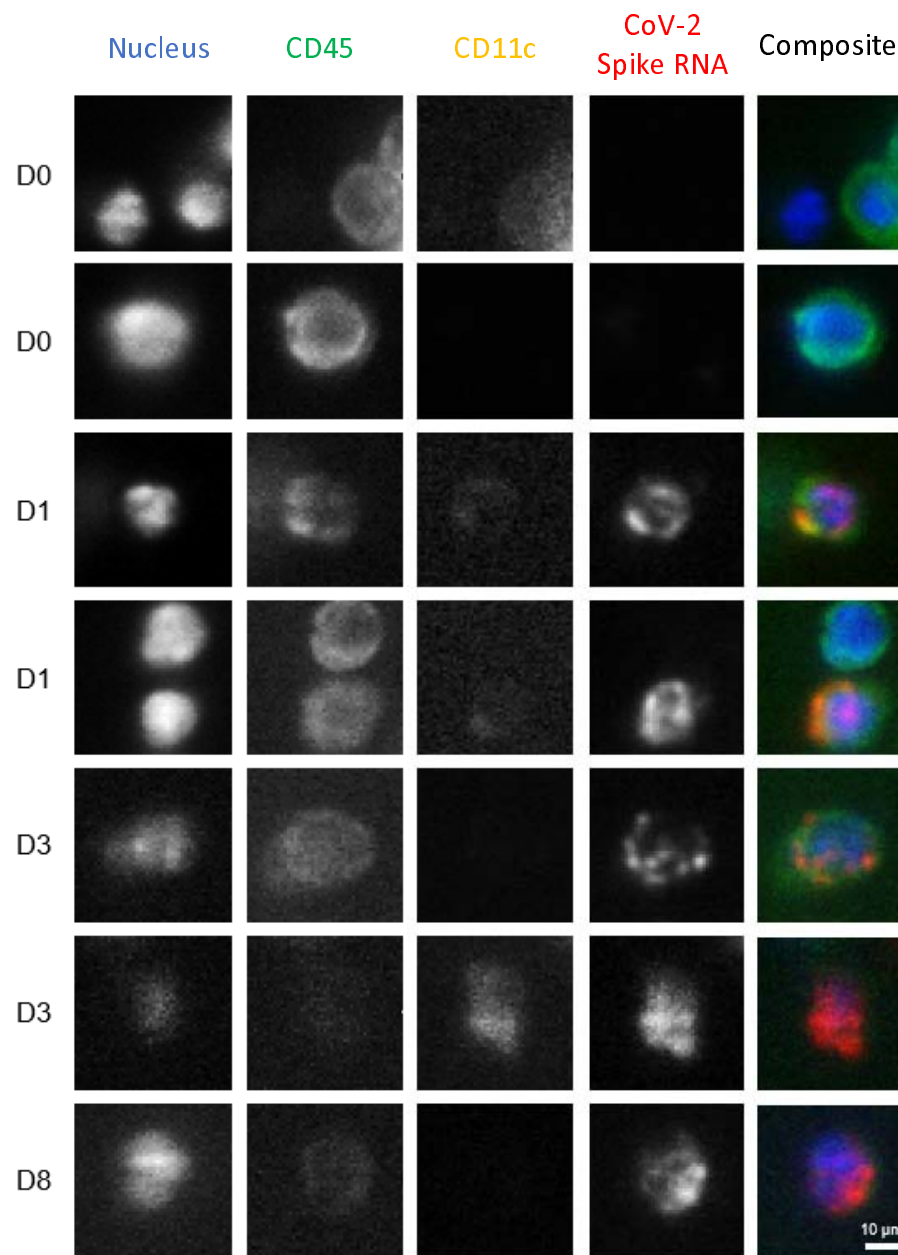


Fig.2

A



B



C

	Sample ID	Spike RNA +	Nuclei	Ratio	Averages
Day0	M1	0	2571	0.00%	0.00%
	M2	0	1000	0.00%	
	M3	0	1000	0.00%	
Day1	M1	32	2710	1.18%	1.08%
	M2	22	3357	0.66%	
	M3	32	2292	1.40%	
Day3	M1	24	2606	0.92%	1.27%
	M2	28	1822	1.54%	
	M3	56	4117	1.36%	
Day8	M1	15	6114	0.25%	0.28%
	M2	10	2450	0.41%	
	M3	2	1183	0.17%	